Unusual Pressure-Induced Phase Behavior in Crystalline Poly(4-methylpentene-1): Calorimetric and Spectroscopic Results and Further Implications

S. Rastogi,*,† G. W. H. Höhne,‡ and A. Keller§,||

The Dutch Polymer Institute/Eindhoven Polymer Laboratories, Eindhoven University of Technology, P.O. Box 513, 5600MB Eindhoven, The Netherlands, Department of Physics, University of Ulm, Albert Einstein Allee 11, D-89069 Ulm, Germany, and Department of Physics, University of Bristol, Royal Fort, Tyndall Avenue, Bristol BS8 1TL, England (U.K.)

Received August 3, 1999

ABSTRACT: The polymer poly(4-methylpentene-1), P4MP1, displays an unusual pressure−temperature (*p, T*) phase diagram raising also issues of wider generality for the phase behavior of single-component condensed matter systems. Previous exploration of this phase behavior through X-ray diffraction has been extended through high-pressure calorimetry, Raman spectroscopy, and time-resolved in situ X-ray scattering. As a result the *p, T* phase diagram, previously postulated on structural evidence is now supported by heat effects defining phase transitions of first order along the appropriate *p, T* phase lines with signs which are self-consistent in accord with the unusual nature of some of the transitions involved. The latter include (1) amorphization under pressure, (2) ordering on heating and disordering on cooling, and (3) sign inversion of the pressure coefficient of the melting point, dT_m/dp, with increasing pressure. The newly recorded heat effects, consistent with the above, include exotherms on amorphization and endotherms on crystallization. The most salient features of the phase diagram involving effects 1−3 are as follows: (α) a re-entrant melt phase region and (β) the assertion that the amorphous material can be compressed to smaller volumes than the crystals. While seemingly counterintuitive, pertinent historical precedents are being quoted. All the above conflicts with the tenets of the widely held Kauzmann restrictions ("paradox"), which it seemingly invalidates. A possible way to reconcile this conflict is by invoking a theoretical explanation on metals existing in the literature. In structural terms, high-pressure Raman spectroscopic and time-resolved X-ray scattering evidence have been obtained. Further issues arising such as the distinction, or otherwise, between fluid and solid "amorphous" phases and their incorporation into phase diagrams are being discussed, and the still open-ended question concerning the molecular nature of the pressure generated amorphous material is being raised.

1. Introduction

The polymer poly(4-methylpentene-1) or poly[(2-methylpropyl)ethylene], abbreviated to P4MP1 as used in the preceding works,[1,2] has the previously defined tetragonal crystal structure comprising two helical chains per unit cell with seven monomer units per two turns ($2 \times {}^7/_2$ helix), a low packing fraction of 0.57, and a melting temperature, T_m, at atmospheric pressure around 245 °C. The amorphous phase at room temperature, in contrast, has a packing fraction of 0.59 and molecules with a close to random coil conformation. It has a glass transition temperature (T_g) in the range 45−50 °C. This means that below T_g the calculated crystal density is lower than the amorphous density. Somewhat above T_g, the usual density relationship between melt and crystal exists.

In the preceding works[1,2] the temperature (*T*)−pressure (*p*) behavior of P4MP1 was explored through in situ X-ray diffraction. In the course of it an unusual phase behavior was observed and mapped which we believe should be of interest not only for polymers but also for condensed matter, in general. In the previous work, changes in the X-ray diffraction pattern were followed both as a function of *T* (at constant *p*), and a function of *p* (at constant *T*). A result of such X-ray diffraction studies along isobaric and isothermal pathways, the broad outlines of a phase diagram, shown by Figure 1, could be mapped. The salient features from the studies are as follows: (1) disordering of the initially

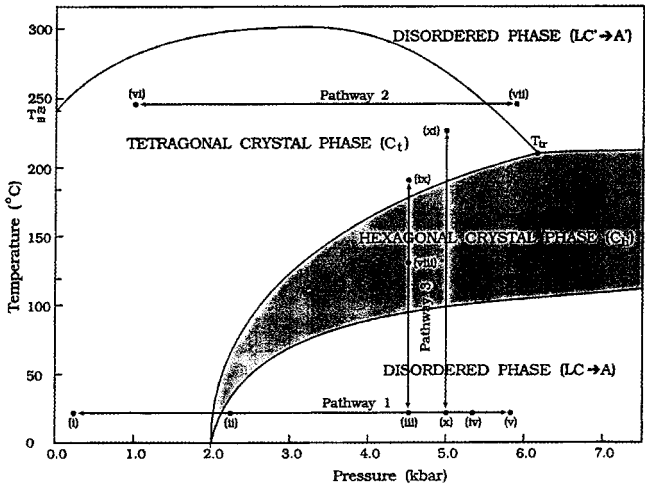

Figure 1. *p*−*T* phase diagram of P4MP1 as obtained by X-ray diffraction[1,2] along isothermal and isobaric pathways, some of which are indicated in the Figure (for detailed notations see refs 1 and 2). The phase ranges include a high-*T* disordered phase (liquid melt), the usual tetragonal crystal phase, and a second low-temperature disordered phase (amorphous glass) representing melt re-entry. The two melt regions are separated by the intervening second crystal phase region (shaded) provisionally identified as hexagonal.

* To whom correspondence should be addressed.
† Eindhoven University of Technology.
‡ University of Ulm.
§ University of Bristol.
|| Deceased.

10.1021/ma9912958 CCC: $18.00
Published on Web 12/08/1999

crystalline material on the application of p at ambient T (pathway 1), the effect being reversible; (2) reversible disordering (in this case, melting) of the crystalline material on application of pressure within the atmospheric p melting region (pathway 2), noting that, in this case, the amorphization (melting) p was significantly higher than for that effect in point 1 above. By this X-ray evidence, the combination of effects 1 and 2 can be interpreted as a re-entrant melt phase at the lower T. Effect 2 in itself implies a maximum in T_m with p, which was attributed to an inversion of sign of the difference in volume between crystal and amorphous (melt) phases, i.e., the ΔV term in the Clausius−Clapeyron equation expressing the p dependence of T_m, itself arising from the inherently higher compressibility of the melt compared to that of the crystal. (3) The existence of the melt phase re-entry could be demonstrated directly by following isobaric structure changes with T at suitably elevated pressures (pathway 3). Here crystal formation on heating and disordering ("amorphization") on cooling was observed. These effects were also reversible. The reversible nature of the transition was observed, provided that a sufficiently broad T interval was spanned (see effect 4 below). (4) A new hitherto unrecorded (provisionally identified as hexagonal) crystal form of P4MP1 was identified with a phase region between that of the usual tetragonal form and the re-entrant disordered (amorphous) region. There was only one-way entry into the hexagonal phase region with T, namely on heating from below but not on cooling from above. Nevertheless, once in the hexagonal phase on raising T further (along pathway 3) a transformation from the hexagonal to the tetragonal form occurred, with the latter disordering directly on subsequent isobaric cooling without an intervening tetragonal to hexagonal transformation. However, the hexagonal phase, once entered by heating from below, was retained on subsequent cooling.

The novelty of the above-described effects, appropriately discussed in refs 1 and 2, will be self-evident, clearly calling for further extension of the investigation both from the point of view of thermodynamics and structure. High-pressure differential scanning calorimetry (HPDSC) has been reported in a separate paper by us.[3] The primary purpose of this paper is to identify the phase transitions, previously indicated by the X-ray diffraction effects, through heat effects as recorded by DSC and through this to assess how far the structure changes, as identified by X-ray diffraction, correspond to genuine thermodynamic transitions. Primarily, are there any heat effects associated with the structure changes and if so is heat absorbed or evolved (endo- and exothermic respectively), and this in accordance with the postulated phase diagram. In addition, some further structural investigations will be reported, invoking vibrational spectroscopy as a first step toward the identification of the molecular changes associated with the unusual phase transitions.

2. Experimental Section

The $p-T$ phase diagram of P4MP1 was investigated with the help of HPDSC. In addition the conformational changes below the T_g were followed in situ with the help of Raman spectroscopy and time-resolved wide-angle X-ray diffraction as presented in this paper.

The material used for the investigation in both cases was the homopolymer isotactic P4MP1 from an industrial source having a melting temperature of approximately 245 °C and a heat of fusion of about 40 J/g at atmospheric pressure (3.45 kJ/mol, 65% crystallinity). Molecular weight and Molecular weight distribution, by information as provided, were M_w = 250 000 and M_w/M_n = 4.0, respectively.

The calorimetric measurements were carried out on unoriented melt crystallized samples using a high-pressure differential calorimeter constructed at the University of Ulm.[4] The high-pressure cells (which can be connected to a commercial power compensated DSC) allow measurements in the T region from room temperature to 300 °C at p values up to 5.5 kbar (550 MPa). Samples of mass = 7−12 mg were hermetically enclosed in aluminum pans against the pressure medium of silicon oil. The heating rate was 20 K/min.

The pressure apparatus enabling in situ Raman spectroscopy was similar to that of Hikosaka and Seto, used in the preceding works.[1,2] The maximum pressure attainable in the set up was 6 kbar. The temperature could be varied from room temperature to 300 °C. A Dilor XY triple monochromator spectrometer, coupled with a liquid-nitrogen-cooled CCD detector, available at van der Waals Zeeman laboratory at the University of Amsterdam was used for recording of spectra with an argon laser, of wavelength 488 nm. Each spectrum was recorded in backscattering mode, after attaining the desired $p-T$ conditions. The time of data collection for each spectrum was 5 min.

Some in situ wide-angle X-ray scattering (WAXS) studies were also carried out in order to provide continuity and overlap between the previous works and the present calorimetric−spectroscopic investigations. In the first place the work was aimed to ensure that the previous, rather unusual effects were reestablished as a preliminary to the new investigations, and following this, a more detailed and quantitative X-ray recording was undertaken in the $p-T$ range of relevance for the new calorimetric study. The same Hikosaka-Seto pressure apparatus was used as had been used in refs 1 and 2. Also, as in refs 1 and 2, the P4MP1 sample was in the form of an oriented film for yielding X-ray patterns with enhanced information content. However, in this case a synchrotron X-ray source at the European Synchrotron Radiation Facility (ESRF), Grenoble, France, was used at station ID11-BL2. Each diffraction pattern was recorded for 30 s on a two-dimensional Princeton CCD detector. Monochromatic X-rays of wavelength 0.08 nm were used, for higher transmittance through the diamond windows.

In what follows, first the new DSC findings as in ref 3 will be combined with the pertinent X-ray, evidence, both from refs 1 and 2 (Figure 1) and of the newly obtained results (Figures 3 and 4) paralleling the present DSC study (Figure 2). Subsequently, the results from vibrational spectroscopy will be presented (Figures 5 and 6), all of it to be followed by a comprehensive discussion.

3. Results and Discussions

In the DSC study, either the temperature was varied at a preselected constant pressure or the pressure was varied at a chosen constant temperature, and the T and p values of endotherms and exotherms that could be identified in the DSC curves were registered. The results are plotted in Figure 2, and caloric data are mentioned in ref 3. The close resemblance between Figures 1 and 2 is apparent, immediately suggesting that the DSC peaks correspond to the structure changes registered by X-ray diffraction hence that the latter are phase transitions. Both show the same subdivision into phase regions within the $p-T$ plane with the boundaries having similar shapes. Also the corresponding numerical values for p and T are similar, which is highly reassuring bearing in mind that the phase lines in Figure 1 were inferred from comparatively few data points obtained by X-ray diffraction. In view of this, the phase diagrams as obtained by X-ray diffraction (Figure 1) and by calorimetry (Figure 2) can be regarded as

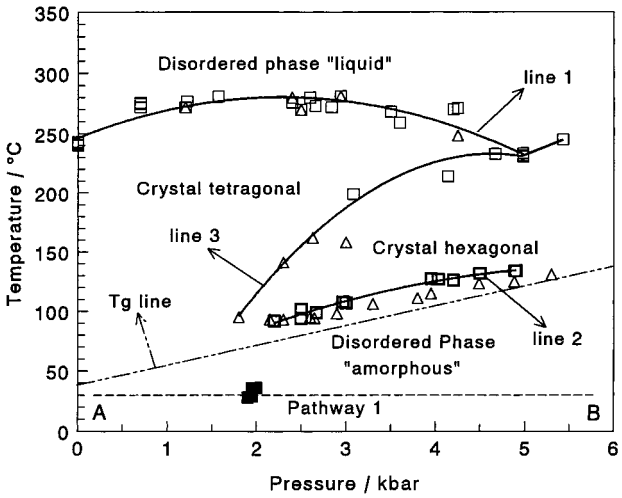

Figure 2. $p-T$ phase diagram of P4MP1 as obtained by DSC calorimetry. Open symbols represent peak positions of endotherms; filled symbols (●) correspond to the exotherm along pathway 1. Open squares (□) refer to endotherms obtained on first heating at fixed pressure, whereas open triangles (△) refer to endotherms obtained on reheating the sample cooled from the melt. The dashed line is the T_g line, drawn from the data obtained from ref 5. Thermodynamic details on the figure are provided in ref 3.

practically identical, which we regard as one of the principal outcomes of this study.

In the following sections, the various phase regions and associated phase transitions will be discussed. It is to be noted that the interpretation and discussion to follow are based on the heats involved in the endotherms and exotherms and on the associated T and p values and on their signs. Establishment of a heat balance in terms of the actual amounts of heat involved is not attempted in this paper, which is undoubtedly an open issue requiring further investigation.

A final comment concerns the term "phase diagram". Commonly it refers to the areas of existence of the various phases and their boundaries, as governed by equilibrium thermodynamics. Semicrystalline polymers are never in equilibrium, best documented by the fact that they violate the phase rule. True phase diagrams of polymers are thus rare, and they are most often obtained by extrapolation from data on semicrystalline polymers. Experience tells us, however, that the non-equilibrium phase diagrams obtained by direct plotting of data gained from semicrystalline sample have largely parallel phase boundaries to the equilibrium diagram, although usually shifted by 10−20 °C to lower temperatures. They, thus, can be used as a good insight into the expected equilibrium phase.

3.1. Disordering with Increasing Pressure below the Glass Transition Temperature (T_g). Figure 3 shows a series of in situ X-ray diffraction patterns of an oriented, crystalline film of P4MP1 at increasing pressures up to 2.6 kbar, all at a constant temperature (25 °C which is below $T_g \cong 45$ °C). It is reported that in P4MP1 the glass transition temperature increases at a rate of 15 °C/kbar.[5] The covered range of pressures as shown in Figure 3 of this paper reaches midway to the prior series of diffraction patterns shown in Figure 3 of ref 2. Here it is now documented in closer steps. Comparison between the two sets of experiments shows that the effects observed are similar. Specifically, the pronounced broadening of the reflections and consequent loss of definition in detail sets in at around 2 kbar. The equatorial, intense 200 reflection of the original tetragonal structure remains comparatively sharp and highly oriented. Nevertheless, it splits into a doublet at the stage where overall line broadening occurs over the rest of the diffraction pattern. Despite the loss of the definition in the reflections at around 2 kbar, the fiber periodicity is retained, as is apparent from the preservation of layer lines, the most intense off-equatorial reflection of which is 212 in the original structure. It remains an intensified blob in the same region and marks the 2nd layer line (Figure 3a in the present paper and also in the earlier paper).[2] This is true even when all other reflections are lost, except for the split equatorial 200 reflections (Figures 2d, 3c and 3d in the earlier paper).[2] In anticipation of the following discussion, it can be stated that the material has become disordered with retention of the original chain orientation. The chains remain parallel, implying a straight-line progression of monomer units, and this in their crystallographic conformation and in at least some close range order between chains. The latter means that some regularity in chain packing is preserved in the *ab* plane as well as in the orientational and translational packing of the chains.

The method of recording of the X-ray pattern in the present work has allowed a more quantifiable display of the diffraction results. For this, the intensities along the original arc-shaped reflections in the fiber patterns of Figure 3, were spread uniformly along full circles by performing integrations. The radial traces so generated are shown in Figure 4. Even if by such averaging one loses the substantial amount of information that is inherent in fiber patterns, the disordering effect of the pressure is more apparent in Figure 4 than in Figure 3. The crystalline nature of the reflections is seen to be lost at around 1.9 kbar. In fact, the trace for 2.6 kbar by usual criteria can be considered as an amorphous pattern. Even the remaining equatorial doublet in the original oriented pattern is showing up only as a pair of broad humps (between $2\theta = 4-6°$). Except for this latter doublet, the pattern is essentially similar to that of the noncrystalline atactic P4MP1.[6] In specific detail, the 200 reflection remains comparatively sharp up to about 1.9 kbar, shifting slightly to higher angles while the position of the prominent other reflections hardly changes. This is consistent with lateral compression of the unit cell along the *a* axis, as expected. Figures 3 and 4 reveal the changes also in the other reflections visible, namely 212, 321, and 420 before their eventual broadening and merging into a halo at around 1.9 kbar. It is to be noted that the changes are largest in the *hkl* reflections, 321 and 212, compared to *hk*0. The 312 reflection vanishes before the others, and the 212 reflection drastically broadens, with its intensity reduced.

Our first announcement of "amorphization" by pressure applies to the process just described. It must be remembered that the transformation occurs below T_g; i.e., the large-amplitude, cooperative conformational motion in the amorphous defects as well as at the interface to the crystals is frozen, and chain reorientation and translation are similarly impossible. The observation must, thus, be described as local disordering, keeping much of the orientational and translational correlation. The subsequent experiments of Okumura et al.[10] display in their published X-ray diffraction patterns in their Figure 3 the same features of pressure-

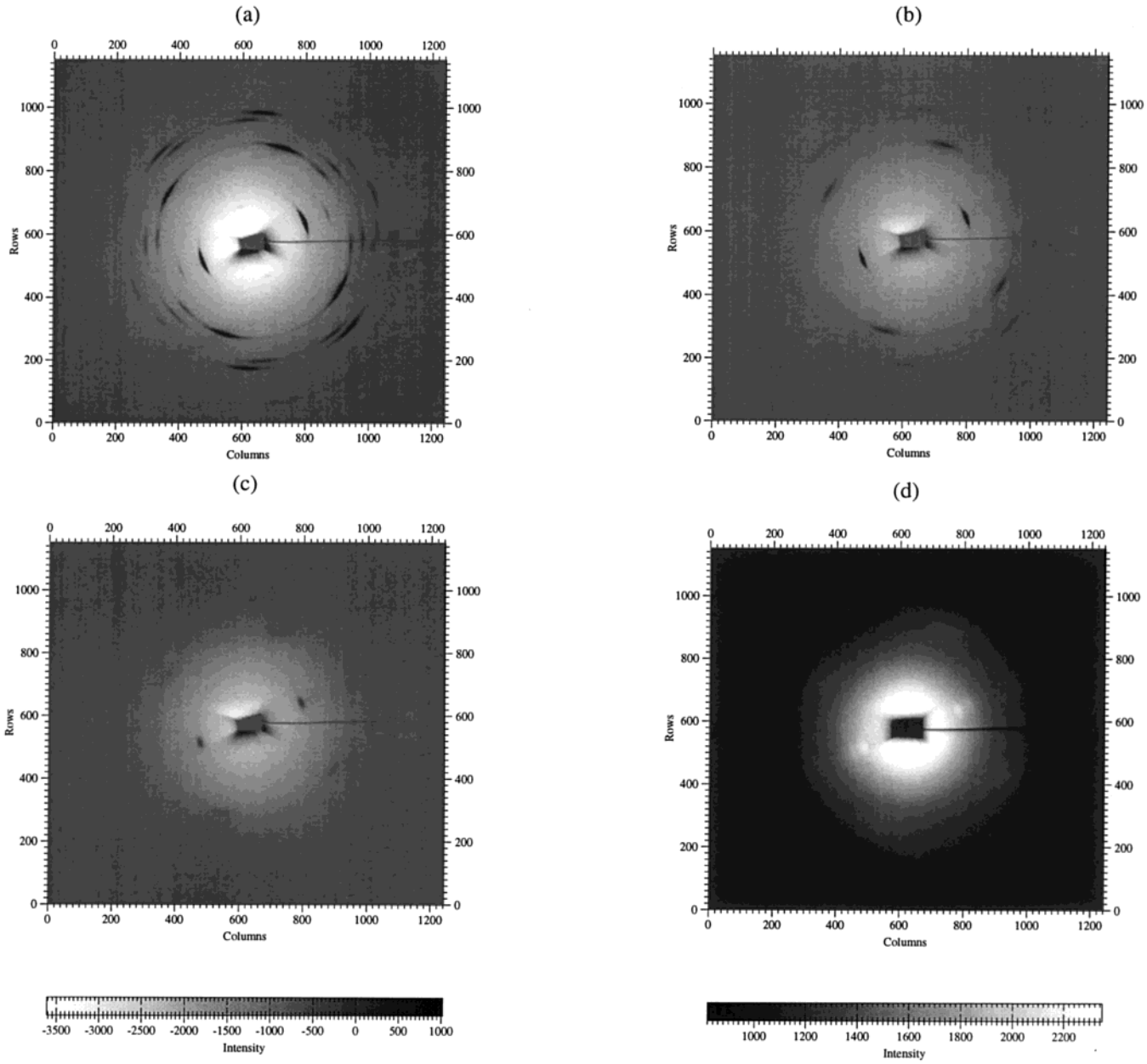

Figure 3. 2D X-ray patterns of P4MP1 melt crystallized oriented sample as recorded on the CCD detector, in situ at three different pressures at the room temperature (25 °C): (a) at atmospheric pressure; (b) at $p = 1$ kbar; (c) at $p = 2.0$ kbar; (d) at $p = 2.6$ kbar. To observe the doublet along the equator, the contrast has been changed.

induced disordering. With the above, more detailed definitions of disordering, we must assume that the "disorder of the first kind" that Okumura et al. suggest and our "amorphization" are referring to the same effect with differences being caused by varying degrees of shear stress, crystallization, and sample origin.

At this point it is worth making a distinction between cooperative motion realized during drawing process of an isotropic film of a polymer below the T_g and the one mentioned above. In the present study, on application of pressure, i.e., on application of compressive stress, the compressive strain either does not exist in hydrostatic conditions or is very much smaller than the tensile strain a polymer experiences during the drawing process. In the process of compressive stress, since volume of the bulk decreases, the glass transition of the semicrystalline polymer increases which further hinders chain mobility and thus cooperative motion of the chains within confined bulk. However, in the case of the drawing process, the polymer is forced mechanically to deform and long molecules are drawn in a preferred direction, thus allowing the cooperative motion for orienting chains in the draw direction.

More detailed evidences for disordering by means of pressure below T_g have been reported above. We can now turn to the interpretation of calorimetric measurement along pathway 1. As indicated in Figure 2, there is a heat evolution effect (an exotherm) recorded at 2 kbar. This signifies, in the first place, that there is a genuine phase transition setting in at that pressure and, second, that the transition is exothermal, (Figure 3, in ref 3). The heat evolved is small in magnitude (0.9 J/g) compared to a standard endothermic melting peak at the usual higher melting temperature (10−40 J/g for our material depending on pressure and thermal history). Yet it is reproducible along pathway 1, both with respect to the p region where it is setting in and with respect to its exothermic nature. In terms of both

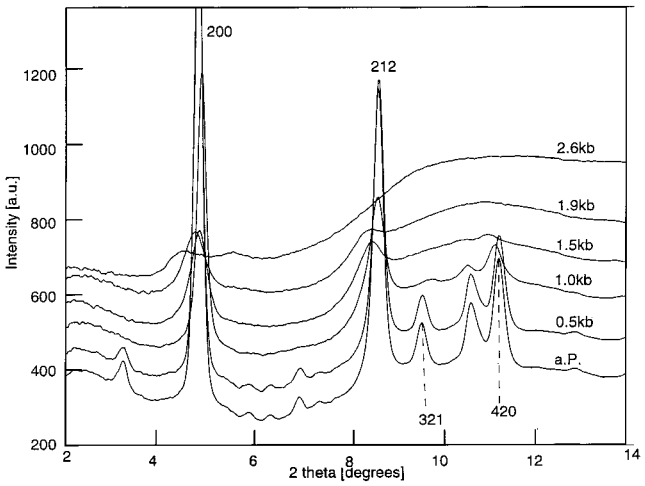

Figure 4. Radial intensity traces of X-ray diffraction patterns along the scattering such as in Figure 3 after azimuthal averaging (integration) of the reflections over their respective full circles (without Lorenz correction for the azimuthal angle which, while needed in principle, would not affect the points at issue). X-ray wavelength: 0.08 nm.

position and sign this is consistent with the phase diagram of Figures 1 and 2. With a re-entrant melt phase and associated inverse melting in particular to feature in more detail in the discussion, even if the small magnitude of heat evolved (or absorbed) may leave room for alternative interpretation (see ref 3).

To further investigate the nature of the disordered phase at the molecular level, we resorted to in situ vibrational spectroscopy. Raman spectroscopic measurements were carried out along pathway 1 of the $p-T$ phase diagram, Figure 1. Spectra recorded at different pressures at the room temperature are summarized in parts a−c of Figure 5. Noticeable changes are observed in the spectral regions of 200−500, 750−860, 1100−1200, and 1400−1450 cm^{-1}. The most intense peak, at 1330 cm^{-1} in Figure 5c, is a known phonon vibration peak from the carbon atoms of the diamond windows of the pressure cell. When required, this can be used as an internal calibrant for intensity and peak positions.

Taking the above spectral regions in turn, we can make the following observations. The band at around 400 cm^{-1} shows gradual but pronounced broadening with pressure. So does the group of bands in the 750−850 cm^{-1} region, but here the brodaning is combined with an inversion of the intensity ratios of the low and high wavenumber peaks at around 770 and 840 cm^{-1}, respectively, making the changes induced by pressure rather conspicuous. Also the whole doublet region is shifting continuously to higher wavenumber with increasing pressure. There is at least a trend of the same in the doublet at 1150 cm^{-1} where the initially unequal doublet components equalize in height with increasing p until coupled with the effect of broadening the two peaks merge. The same effect is seen for the band groups at around 1430 cm^{-1}. The exception here is that it is the higher wavenumber peak of 1437 cm^{-1} which is smaller at atmospheric p and increases with p in the direction of becoming equal to the lower wavenumber peak 1425 cm^{-1} to give an apparently single broad band at 2.5 kbar.

Separately, a heating experiment was performed at atmospheric p, and the Raman spectrum was recorded. As expected, all bands broadened because of the less-structured spectrum of the melt. Even so, a specific

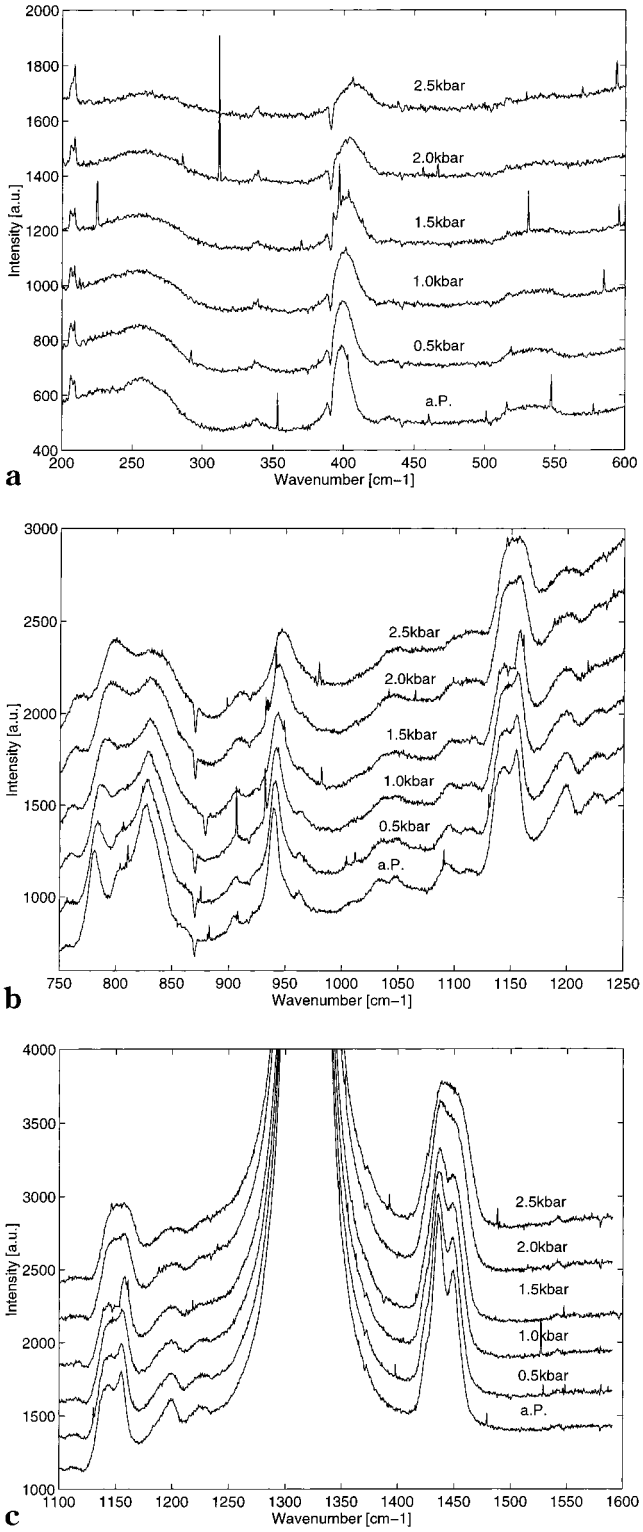

Figure 5. Raman spectra of P4MP1 as recorded in situ with increasing pressure along pathway 1, Figure 1. a−c represent three different spectral regions

change on melting could be detected in the band groups around 800 cm^{-1} as shown by Figure 6. Comparison with Figure 5b indicates that this change is of the same nature as that induced by increase of p in the same spectral region. It is, namely, an inversion of the intensity ratios of the extreme peaks of the group and a shift toward higher wavenumbers in addition to overall broadening. It thus appears that the genuine melt, as produced by heating, has at least some spectral

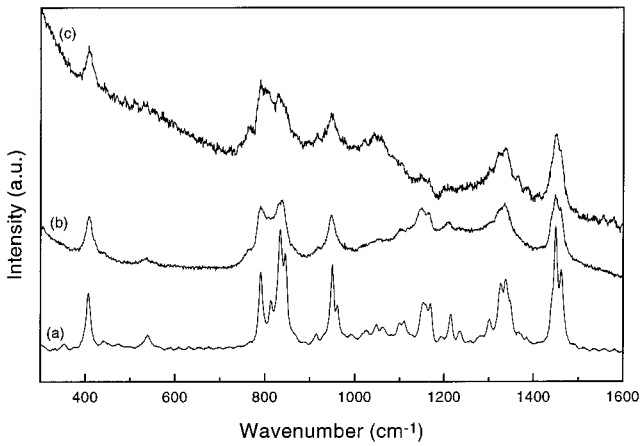

Figure 6. Raman spectra of a P4MP1 recorded at atmospheric pressure at three different temperatures: (a) at room temperature, (b) at 240 °C ,and (c) at 245 °C. The spectrum shown in part c has similarities to that obtained above 2 kbar in Figure 5.

features in common with the material produced through disordering by pressure.

In addition to the above description, a specific attribution to molecular groups and motion would of course be desirable. The known spectroscopic background of P4MP1, however, is not well established. From what is known,[7,8] we can say the following concerning the above band regions. The 1400−1500 cm^{-1} region is stated to be associated with side chain atoms, while all the others featured above are mixed bands with contributions from both side chain and main chain groups. The infrared bands at 809 and 844 cm^{-1} in isotactic P4MP1 are sensitive to tacticity and crystallinity.[7] From the normal-mode analysis, similar conclusions were reached by Bahuguna et al.[8] In our work on Raman spectroscopy, the bands closest to these should feature in the region 750−850 cm^{-1}. Thus, considering the use of two different techniques, Raman and IR, changes marked in the bands within this region may be associated with changes in the crystals, specifically crystallinity. Since it has not been feasible for us to acquire atactic P4MP1 and to quench isotactic P4MP1 in its glassy state, we have followed this cautious approach.

It follows that lacking further information the best we can do at this stage is to attribute the Raman spectroscopic effects featured above to the side groups of the P4MP1 chain.

It would follow therefore that the main influence of the pressure is to affect the conformation, and through this the packing of the side groups. This seems to be most plausible not only by a priori considerations but also by the available X-ray diffraction evidence and by the very low entropy change measured along pathway 1. Namely, as already stated, in the disordered material even after 3-dimensional lattice order is removed, signs of the original layer line periodicity along the chain direction are retained. All this indicates that the chain backbone has remained in its unaltered conformation as it had been in the crystal, at least over a length corresponding to a very few crystallographic repeats. This in itself focuses attention to the side groups as the sites of change and source of disorder as produced by application of pressure. This line of reasoning raises further issues regarding the requirements to create a truly random structure and, conversely, further issues as to the nature of the genuine melt, questions we cannot answer at this stage even if we shall return to them in the discussion.

3.2. Inversion of the Pressure Dependence of the Melting Point. It was inferred from X-ray diffraction studies along pathway 2 (Figure 1), that the melting point, after an already established initial rise[9,11] ($p \sim 3$ kbar; $T \sim 300$ °C) must pass through a maximum and then it must decrease on further increase in p (see refs 1 and 2). This effect is attributed to change in sign of ΔV in the Clausius−Clapeyron equation, ($dT_m/dp = \Delta V_f/\Delta S_f$). The phase line in ref 2 (present Figure 1) was drawn on the basis of ref 9. The authors, in ref 9, mapped T_m as a function of p. In the course of this a dT_m/dp of 42 K/kbar was observed up to 0.7 kbar. Beyond 0.7 kbar dT_m/dp gradually decreased to 10 K/kbar at 1.8 kbar, the upper p limit of these measurements (our measurements: +50 K/kbar at low pressure, zero around 2 kbar and −20 K/kbar above 3 kbar[3]). The inversion of Clausius−Clapeyron was confirmed by X-ray diffraction patterns along pathway 2 and that of similar other isothermal X-ray series. As seen from Figure 2, the anticipated maximum in T_m closely follows the T_m vs p line in Figure 1, postulated previously on the basis of X-ray work,[1,2] even if at slightly lower T values.

Preceding the present calorimetric work, the existence of the maximum itself, and the implied sign inversion in the Clausius−Clapeyron equation, has already been established by other works elsewhere[10] undertaken in the light of our first X-ray findings.[1,2] The actual T values, however, are substantially lower than anticipated by us through Figure 1 and presently confirmed by Figure 2. Without invalidating the underlying basic principles, we believe that the reason for the numerical discrepancy is likely to lie in the use of a different starting material, obtained from two different sources. Differences in dT_m/dp for P4MP1 originating from two different sources were also observed earlier.[9,11] The polymer used in ref 9 had a higher melting point at atmospheric pressure than the one used in ref 11, because the polymer used in ref 11 was a copolymer.

3.3. Transitions Involving the Pressure-Induced Disordered Phase and Further Phase Effects. In the preceding section, the heat effects observed along pathway 1 of Figure 2 established that the disordering by pressure corresponds to an abrupt and reproducible change and may be an indication of a possible first-order phase transition, as revealed previously by X-ray diffraction (Figure 1 and refs 1 and 2). Hence the disordered ("amorphized") structure corresponds to a distinct phase. The two points of the phase boundary in Figure 2 are insufficient to complete the phase area of the low-pressure side. According to the prior X-ray studies, this phase is bounded at the high T side by a crystalline phase along line 2 in the phase diagram. This is nevertheless different from the commonly observed tetragonal structure of P4MP1 and that, on the information available to us, identified as hexagonal, with a one-way entry, i.e., by heating only, with temperature.

The previously postulated phase line 2 could now be identified by calorimetry, displaying a small but clearly identifiable endotherm of 1.5 ± 0.3 J/g on isobaric heating.[3] Normally an endotherm observed on heating would signify an increase of entropy as in melting of crystals. As follows from the X-ray patterns, this does not seem to be so in the present case, namely that we

are passing from disorder to crystalline ordering, in this case to the newly recognized hexagonal crystal phase.

Previous X-ray evidence summarized in Figure 1 proved that one could regain the tetragonal structure on further isobaric heating, which, in turn, converts into the melt at its appropriate T_m along line 1. The DSC work, on continued heating along the isobaric pathway, at first only gave the endotherm when crossing line 1 of 10 to 40 J/g, the normal heat of fusion, which obviously depends on the pressure and thermal history of the sample.[3] Nevertheless, a heat effect in the form of a small endotherm (<1 J/g and thus not easy to detect in every experiment) did become apparent after the melt thus obtained isobarically at the corresponding elevated pressure had been cooled back to room temperature and then reheated again along the same isobaric pathway. In this case, two successive small endotherms were recorded, one close to line 2 and a second one on crossing line 3, followed by a large ultimate endothermic melting peak along line 1. Combined with the X-ray experiments these successive three endotherms correspond to the transitions: disordered ("amorphous") → hexagonal crystal (C_h), hexagonal (C_h) → tetragonal crystal (C_t), tetragonal crystal (C_t) → melt (liquid) phase transitions, respectively. These heat effects quantify Figure 1 with calorimetry and permit a thermodynamic discussion.

To note, in Figure 2 the data obtained on the first runs (□) are distinguished by notation from those obtained in the second and later runs (Δ). As can be seen, the effects along line 1 are closely reproducible. In the case of line 2, the peak positions arising on the second run fall slightly below the ones obtained in the course of the first run while still defining line 2, here shifted slightly downward in T, but with the same endotherm. Regarding line 3, this arises largely from second and subsequent runs. The reason for the latter must lie in differences in the kinetics of the phase transformation, the amount of phase transition from hexagonal (C_h) to tetragonal (C_t), and the sharpness of the transitions, which all are influenced by the route taken. Also note that line 2 is approxiamtely parallel to and above (Muller and Pieteralla; University of Ulm, private communication) the T_g vs p line, a point we shall return to in the general discussion.

A further, more significant feature is the intersection of lines 1 and 3 in Figure 2. This terminates the existence of the tetragonal phase at higher pressure. This would correspond to the tetragonal−hexagonal−liquid triple point in Figure 1. The additional single, yet well-established new calorimetric datum point, at 5.5 kbar in Figure 2, now confirms this previous attribution. It also shows how the new hexagonal crystal phase intervenes. Hence, it interrupts the continuity between the high-temperature liquid and the low-temperature disordered, "amorphous", phase (the nomenclature here becomes ambiguous; any distinction, such as may be justifiable, between liquid melt and solid "amorphous" phases will be discussed in the section General Discussion).

The signs for the heat effects deserve special consideration. As already stated, an endotherm, i.e., heat absorption on crystallization, is contrary to the conventional experience. Nevertheless, it is consistent with the crystallization occurring from a re-entrant melt phase on raising of temperature. As already discussed in ref 2 such a re-entrant disordered phase implies a higher entropy (S) for the crystal compared to that of the disordered ("amorphous") phase at the low temperature. Counterintuitive as this may appear at first sight, it is certainly permissible and possible (see refs 1 and 2 and Figure 7 in this paper). This means a positive ΔS on crystallization, which also means a positive enthalpy ΔH and hence an endotherm (by accepted sign convention). This effect, already inferred from X-ray diffraction, has thus been substantiated by the present calorimetry: thus consistency between both the position (in the p and T plane) and the sign of the heat effects between the X-ray and calorimetry data has been attained.

In the preceding X-ray work,[1,2] in addition to crystallization on heating, also the inverse, namely disordering ("amorphization") on cooling was directly observed, and in fact, it was presented as the most conspicuous feature of melt phase re-entry. From this, a corresponding exotherm would be expected on cooling. Unfortunately we could not detect any heat effect on isobaric cooling through lines 3 and 2. We know from the X-ray diffraction results[1,2] that the hexagonal phase region cannot be re-entered on cooling; hence, we would not expect phase line 3 to become apparent on cooling by calorimetry either, which is in accord with the present DSC results. We would expect, nevertheless, a tetragonal crystal → disordered ("amorphous") phase transition. However, we do not know where such a tetragonal → disordered ("amorphous") phase line (on cooling) is situated in the phase diagram. The transition may well be too broad due to kinetic reasons for the comparatively small heat effect (which should be an exotherm in this case) to be registered in our DSC experiment. The possibility of an exotherm which remains undetected on cooling seems very likely as the appearance of an endotherm on second heating run,[3] close to line 2 shown by Δ in Figure 2. These observations suggest that the cooled tetragonal crystals at the elevated pressures must have transformed to the disordered ("amorphous") phase on prior cooling.

While missing the calorimetric information relating to the disordering on cooling, the data, such as we possess, are self-consistent. The isothermal disordering ("amorphization") along pathway 1 is exothermic in nature, which is to our knowledge the first instance of an exothermic heat effect on disordering. The heat given off along pathway 1 is then regained (hence endotherms) in two stages in the course of crystallization as we traverse phase lines 2 and 3 in Figure 2 successively on isobaric heating with the usual large heat absorption (i.e., endotherm) on final melting (line 1).

The newly uncovered, provisionally assigned hexagonal crystal phase, while not the focus of the present paper, commands interest in its own right. In the first place, this is because of the unusual nature of its accessibility. To recall, it can only be entered one way with temperature, namely only through isobaric heating, but not through cooling. Further, once entered, this phase is retained irreversibly on cooling and also on subsequent pressure release. As a consequence, this crystal phase can be retained as a metastable phase at room temperature and atmospheric pressure. This latter feature, among others, should facilitate a more in depth crystallographic structure determination. In the present works, concerned mainly with phase behavior, we have not pursued the structure issue further, beyond stating that the chain packing, from the evidence we have, is most likely to be hexagonal with the layer line spacing consistent with a 3/1 helical chain conformation. While

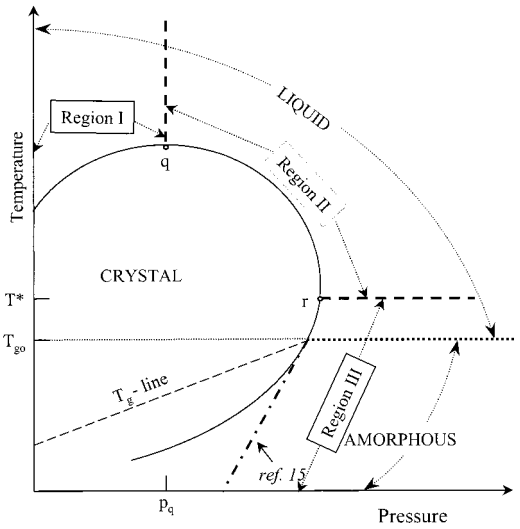

Region I : ("normal")
$dT_m/dp = T.\Delta V / \Delta H > 0$; $\Delta V = V_{liquid} - V_{crystal} > 0$; $\Delta H > 0$; $\Delta S > 0$; (endotherm)

Region II : (densities invert)
$dT_m/dp = T.\Delta V / \Delta H < 0$; $\Delta V < 0$; $\Delta H > 0$; $\Delta S > 0$; (endotherm)

Region III: (entropies invert)
$dT_m/dp = T.\Delta V / \Delta H > 0$; $\Delta V = V_{amorphous} - V_{crystal} < 0$; $\Delta H < 0$; $\Delta S < 0$; (exotherm)

Figure 7. Simplified $p-T$ phase diagram with its thermodynamic implications. (i) In subdividing the "melt" phase into liquid and amorphous, we followed the terminology of Tammann and other thermodynamic textbooks quoting it as cited in refs 1 and 2 (see text). (ii) The intervention of T_g and its effect on the $p-T$ line as shown by the alternative line $- \cdot -$ is our attempt to incorporate Fecht's[16] consideration into a $p-T$ phase diagram.

irreversible on isobaric cooling, this hexagonal phase formation can nevertheless become reversible on isothermal changes in pressure (see X-ray work in ref 2). This may well be the consequence of it being above the T_g, a point to be taken up again in the General Discussion.

4. General Discussion

4.1. The Schematic "Overall" Phase Diagram. In what follows, we shall resort to a simplifying schematization. For this, we are taking the lead from what we consider is possibly the most salient finding of the present work, a low-temperature disordered phase in the $p-T$ phase diagram which can be created and removed reversibly: isothermally by raising and lowering p and isobarically by respectively lowering and raising T. We shall consider that this disordered phase, necessarily of lower entropy than the crystal, has several features common with the liquid phase at high T, which can be regarded as a re-entrant melt phase. In this respect, the newly found hexagonal crystal phase is regarded as an extraneous complication, intercepting a continuous pathway between the high-T (liquid) and low-T (liquid/amorphous—about the distinction see below) phase regions. It will be omitted in the schematization of Figure 7, which is to serve as a basis for further discussion.

We are realizing that some drastic simplifications and/or assumptions are involved in Figure 7. However, our experimental observations by high-pressure DSC support the very thermodynamic nature of the phase diagram, to which we shall come back to later. Apart from the omission of the hexagonal phase, it implies identity of the high- and low-T disordered phases. As far as this can be a point of dispute we wish to refer to the X-ray evidence and Raman spectroscopy of Figures 4−6. Whatever the interpretation of the remaining diffraction features, the 2.6 kbar trace in Figure 4 (and these become considerably more diffuse at the higher p), would be classed "amorphous" or closely so by the usual criteria of a crystalline X-ray diffraction pattern. Even as far as there is a distinction from a true amorphous phase (e.g., a phase line between the similar disordered phases), this need not basically invalidate the scheme in Figure 7. The scheme has the following advantages to offer: it gives an account of our principal findings in terms of a unifying scheme, except for providing a quantitative heat balance, which, however, with potentially broad transitions, in view of the restrictions of high-pressure calorimetry, would anyway be very difficult to achieve. In particular, a lack of balance in entropies is observed along pathway 1 below T_g, in Figure 1 (associated with ΔH of 0.9 J/g) on raising p isothermally, and that along line 1 in Figure 2 (associated with ΔH of 10−40 J/g for our material depending on p and thermal history) on increasing T at fixed p. Alternative models may be possible where the disordered ("amorphous") state may be considered as conformational disordered glass[3].

4.2. On the Unusual Features of the Overall Phase Diagrams and Their Implications. The overall assumed phase diagram (with the additional, i.e., hexagonal, phase omitted) is represented schematically by Figure 7. The overriding feature, the curving back of the p, T phase line with the concomitant inversions in phase behavior, was discussed in both its thermodynamic and historical contexts in ref 2. At this place we shall lift out some further issues of wider generality but not to the same extent covered previously.

First a brief recapitulation: phase diagrams such as in Figures 1 and 2 are within the bounds of phenomenological thermodynamics and have been envisaged by Tammann as far back as 1903.[26] His motivation (by our present reading) was to avoid the issue of p, T phase lines progressing to infinity (seemingly problematic to him at the time) arising from the recognition that there can be no termination of a liquid−solid (i.e., crystal) phase line and hence a liquid-crystal critical point (by current conception because of symmetry breaking). As an alternative, he envisaged possibilities such as phase lines turning back on themselves, forming closed loops or terminating along the p or T coordinate axes or along other phase lines. Tammann[12] obtained the extreme values along such loops, in terms of p and T, (points q and r in Figure 7) through what he termed "neutral line" construction, an argument we have reproduced in ref 2. He was not in a position to quote explicit examples at the time but performed numerical extrapolations from p, T data, as then known, which yielded the a priori envisaged loop-shaped phase lines.[27]

The p and T values required for the following of the looping back of phase lines were, by Tammann's criteria, beyond what could be accessed at that time. Vogel,[14] quoting Tammann's arguments in 1955, says that such extreme values of p and T may only be realized extraterrestrially or within the earth interior. To this we now add that, as far as the present work is to serve as a pointer, the same *seems to have* become achievable presently under laboratory conditions through polymers, in particular such ones as have loosely packed crystal structures (see also below).

To take the schematics of Figure 7 in some detail: There are three regions with a subdivision in region III. The characteristics of each region in terms of change of the principal thermodynamic quantities, namely ΔV, ΔH, and ΔS, are stated within Figure 7 itself. The present text will contain some additional information.

Region I corresponds to the customary behavior of rising T_m with increasing p. It is terminated by the extreme point q. At this point, $\Delta V = 0$. In terms of Tammann, this point corresponds to the intersection of the "neutral line" for V, i.e., loci where $V_{solid} = V_{liquid}$, with the p, T phase line.

In region II, $\Delta V < 0$, i.e., here V for the liquid is smaller than that for the crystal (in Tammann's presentation the V vs p curves for the liquid and crystal have crossed over). This has the result that dT_m/dp, by the Clausius−Clapeyron relation, has a changed sign; i.e., T_m decreases with increasing p. This region II terminates at the extreme point r where ΔH (hence, in equilibrium, also ΔS) is zero. In terms of Tammann this corresponds to the intersection of the neutral line for H (i.e., the loci where $H_{liquid} = H_{crystal}$; in ref 12 the symbol R is used in place of H) with the p, T phase line.

Region III corresponds to the re-entrant melt phase highlighted previously. Correspondingly, here the crystal melts (or becomes amorphous, for the distinction, see below) on cooling, and conversely, the melt (or amorphous) converts into the crystal on heating. As should be apparent, the requirement that $\Delta S < 0$, and hence that the entropy of the crystal be larger than that for the liquid, is concomitant with the existence of a region III and with the melt phase re-entry it signifies.

Our high-pressure DSC (HPDSC) observations on P4MP1 are that with the increasing pressure, heat evolved (ΔQ) during melting of the tetragonal phase decreases exponentially and approaches nearly zero. A sudden increase in ΔQ is noticed at the higher pressures due to intervention of the hexagonal phase (see Figure 7 in ref 3). In this respect, our HPDSC observations support the anticipated heat evolved/absorbed in the phase diagram summarized under Figure 7.

That the last mentioned entropy inversion in region III of the phase diagram in Figure 7 is at first sight contrary to conventional preconceptions has already been commented on in the last section and in greater detail previously in ref 2. In brief, the conventional association of a lower entropy with the higher degree of order in the crystal compared to that in the corresponding liquid only refers to the configurational part of the entropy which usually dominates. There are, however, also other contributions to the overall entropy of a system, such as, e.g., a correlation component. Such contributions can become significant in a loosely packed, but still periodic system allowing a greatly increased number of positional correlations within the system, which otherwise is still retaining its long-range three-dimensional order (i.e., the periodically repeating mean positions of the repeating motif). This latter point, in combination with possible restrictions arising within the disordered version of the same system (e.g., "log jam"), can then yield the entropic sign inversion under discussion for the overall combined system of liquid and crystal.

As already quoted in ref 2, familiar examples of the last mentioned situation include the formation of regular three-dimensional lattices in suspensions of colloidal lattices. The formation of lyotropic nematic liquid crystals from rodlike molecular entities which, in the absence of other interactions (here we have hard-sphere or hard-rod cases), are purely entropy driven (i.e., the ordering is toward the higher entropy). Even if the above examples correspond to two-component systems with the concentration as the pertinent variable, they are illustrating the principles involved. Of course in the case of a single component system with T as a variable purely geometric, the hard body, i.e., the $\Delta H = 0$ condition, is no longer tenable. Hence, in this case, the sign of ΔH and that of the corresponding measured heat effect have to conform to the inverted entropy requirement. This is what the presently reported calorimetric work has verified, at least in those cases where heat effects could be recorded on traversing a phase line within the available detection sensitivity.

To add further information on entropy inversion, especially at low temperatures in the relatively loosely packed lattice with an increase in mechanical forces, such as compressive stress, defects introduced in the lattice cannot be overcome. Thus, entropy of the crystal increases and exceeds that of the liquid/amorphous phase. Fecht and Greer have proposed similar arguments in metallic alloy systems, where defects introduced in the lattice can be also chemical rather than mechanical in nature.[16,17] This has been discussed more in detail later and, in particular, in the Appendix.

4.3. On Fluid vs Rigid Amorphous Phases. It will have been noticed prevoiusly that the disordered phase has been named interchangeably as a liquid or melt on one hand and as amorphous on the other. This ambivalence goes back to Tammann,[12] who called the disordered phase liquid or melt when above the p, T phase line and amorphous when below, clearly implying that in the latter case it was no longer in the fluid state. We shall try to clarify this issue further below. At this point it should be sufficient to say that despite such a difference in state of matter both the liquid (melt) and "amorphous" (solid) regions in the phase diagram correspond thermodynamically to the same structure, but not to the same dynamics, a fact that today is well understood. Liquids or melts possess cooperative large-amplitude motion; solids (crystals as well as glasses) do not. Both liquid and glasses are, however, in today's preferred nomenclature said to have an amorphous structure (note that the characterization of a phase should always include its structure and state of motion, to be complete). Tammann, who was one of the originators of studies on the glassy state was, of course, aware of this distinction, but did however not have sufficient experimental information to properly express the differences in phase relations. From our modern viewpoint a glass, on a finite time scale, represents a nonequilibrium state (even in a noncrystallizable substance) because of excess volume which, for kinetic reasons, it is unable to reduce. Nevertheless, changes in phase stability arising from such a source will be small compared to differences between the crystal and liquid/amorphous phases. Consequently, in what follows, no distinction will be made as to whether the disordered phase is actually a liquid or a glass, and in the latter case, no distinction will be made as to the degree of equilibrium (aging) within the glassy state. While the actual numerical values defining the phase line may slightly be affected, this will not basically influence the overall scheme.

Nevertheless, some questions and uncertainties as regards the relation between phase behavior and vitrification of the amorphous phase have arisen in the present work. Thus, the disordering by pressure at room T (pathway 1) was found to be reversible, both by X-ray diffraction[1,2] and also by DSC (even if no endotherm was detected on pressure release, the exotherm appeared again on reimposition of pressure).[3] Also, the exotherm reappeared again, on application of pressure, after returning to the starting position (ambient $p-T$) following other circuits in p, T space. In contrast, line 2 in Figure 2 was parallel and above the T_g vs p line and even holds further for the second run though at relatively lower temperatures. Purporting to deal with equilibrium phase diagrams, we have been rather dismissive of such a correlation in the preceding section. Nevertheless, the reversible entry and exit into the hexagonal phase on isothermal application of p at T values above T_g (ref 2 and quoted above) suggests that T_g may have an influence after all, at least on the formation of the hexagonal crystal phase. Summing up, it is seen that the influence (or lack of such) of T_g may not be uniquely defined: it may influence some of the phase transitions, while some others may remain unaffected by it.

4.4. Conflict with the Kauzmann Paradox and a Possible Way Toward its Resolution. With the discussion of T_g, the present results are raising a wider and in fact overriding issue, namely the applicability, or even validity, of the Kauzmann paradox,[15] which dominates much of the thinking in the science of the glassy state. In broadest generality basic properties such as V, S, etc. vary more steeply with the thermodynamic parameters p and T in the liquid than in the crystalline solid state. It follows that the V vs p and V vs T curves should cross over, and the same is true for the corresponding S and H curves. In fact this is the basis of Tammann's "neutral" line constructions and the resulting looping back of the p, T phase lines.[12] Now, the essence of the Kauzmann argument is that such a crossing-over is forestalled by the intervention of vitrification. The paradox itself arises when applying it to the change of entropy with T. This not because of the crossing-over itself but because this would lead to negative S values at $T = 0$ K where the entropy of the crystal must be zero (hardly ever spelled out in this form by sources which are referring to it). Now, as a re-entrant melt implies S_{liquid} (or $S_{amorphous}$) $< S_{crystal}$ this means that our results are suggesting the reality of the Kauzmann paradox.

At this point the question to ask is as to whether this is physically permissible. The answer to this is in the affirmative. Of course the entropy cannot become negative, but that does not mean that the situation of $S_{liquid} < S_{crystal}$ cannot arise at T values where both S_{liquid} and $S_{crystal}$ are still finite and positive. It only means that S_{liquid} cannot be extrapolated linearly down to such low T values where its sign would invert. In other words, some further changes will need to occur within the material, which would prevent this.

Thus, if the violation of the Kauzmann paradox is not excluded (as has just been argued), we may still ask whether the validity of the Kauzmann restrictions, so widely held in polymer science, can still be safeguarded even in the light of our present results which seemingly contradict it. Here we invoke a possibility in this direction, which has arisen through a scheme proposed by Fecht[16] in the context of metals. Through this, by our reading at least, the existence of a re-entrant melt phase could be made compatible with the Kauzmann paradox.

In what follows, we shall present the Fecht scheme, and this in a formulation of our own so as to make it potentially transposable to the present work on a polymer and to the line of argumentation followed in the present discussion. The main text here will only give the outlines and principles, the particulars, including a critique, will be laid out in the Appendix.

The essence of the Fecht argument is that below T_g defect-containing crystals can be considered as being in a frozen-in metastable state. Here, phase stabilities and phase transitions as a function of defect concentration (c_d in our notation), with respect to the corresponding "melt" states, can be treated as usual in thermodynamics. The "melt" state can be either a fluid or a glass, in the latter case the Kauzmann restriction being directly taken note of. If the Kauzmann restriction is not taken note of, crossing-over of entropies would occur, just as in Tammann's treatment (not quoted in ref 16) and in our present case, with a concomitant re-entrant melt region. Fecht purports to show that, with the introduction of the defected crystal as a reference state for the crystal double valued melting points, melt re-entry results even with the Kauzmann conditions adhered to. He constructs a c_d vs T "phase" diagram which is of the same shape as our p, T phase diagram, Figure 7, as from p_q onward, i.e., embracing our regions II and III. In fact, we ourselves are representing region III in Figure 7 in the light of Fecht's c_d vs T diagram (Figure 2 in ref 16). That is, in addition to Tammann, we introduce T_{go}, the ideal glass transition temperature, where the slope of the liquid free energy equals that of the ideal crystal. Below this temperature, the liquid state would have a smaller entropy than the crystalline state. This changes the shape of the p, T curve but not its re-entrant character. Also included in Figure 7 is the subdivision of the overall disordered region into a narrow 'liquid' region within the interval $T^* - T_{go}$ and a wider solid glassy region from T_{go} downward, which following Fecht (and indeed Tammann) we term "amorphous", this subdivision, with the appropriate nomenclature, being displayed by our own Figure 7.

The Fecht treatment raises some basic issues and queries. These are laid out in the Appendix. At this junction, we are anxious to make the point that Fecht's and our own motivations are basically different. Fecht is making some theoretical predictions based on a priori considerations, some of which may well need scrutiny. In contrast, we are seeking to explain our experimental results. Such, mutado mutandis, may be provided by the Fecht scheme:[16] hence, we resort to it in the hope that it may serve as a pointer in an attempt to preserve the validity of the Kauzmann arguments, which otherwise would cease to be tenable, at least in their widest generality. Possible weaknesses in the Fecht scheme should not reflect on our own results and deductions directly arising from them.

Even as far as the Fecht scheme has a claim for validity, our paralleling of his c_d, T with our p, T plots still requires comment and elaboration. Here we feel that the line we have taken is not only justifiable but could be positively forward looking. We know from our X-ray evidence that the application of p (e.g., along pathway 1) ultimately produces disorder (amorphiza-

tion) and hence must involve the creation of defects. It is at this point that we can usefully invoke our subsidiary spectroscopic results. These contain two features of significance for the present issue.

(i) There is a gradual change of the Raman spectra (Figure 5) in a direction which points toward the melt state (Figure 6), which is consistent with an associated disorder due to defects. Note that the spectroscopic changes are gradual compared to the more sudden change in the X-ray diffraction pattern and, principally, with the appearance of a discrete heat effect (exotherm), both at around 2 kbar of pressure. We believe that these differences in continuity are significant, because the continuous spectroscopic effects indicate a gradual distortion of the structure, while the discontinuous X-ray and heat effects signal a phase change. It would follow that the structure, while still within the potential well of the same phase, exhibits progressively more defects until a different (here amorphous) phase is energetically preferred. This, in principle is consistent with conceptions on phase transitions in general and with the Fecht defect model below T_g in particular.

(ii) By existing spectroscopic assignment, the structural changes introduced by application of p are confined to the side chains, with the main chain conformation, which by X-ray diffraction is the $^7/_2$ helix, retained. This should specify the nature of the defects involved: a change in conformation, specifically a collapse, of the side groups with resulting changes in the mutual chain arrangement, and in the packing of the chains while the chains are still, at least locally, straight in the $^7/_2$ helix conformation.

4.5 On Pressure- (*p*-) Induced Amorphization: The last mentioned points bring us to the issue of pressure-induced amorphization. As laid out in ref 2, creation of a (solid) amorphous phase through application of pressure, i.e., without going through a liquid melt phase, is being currently observed in a range of largely inorganic substances, such as alloys,[17] silicates,[18] ice,[19−22] phosphates,[23−25] etc. As we tried to categorize this observation in ref 2, these phases fall into two classes.

(i) The first is straightforward lowering of T_m in such amorphous materials where the density of the liquid is higher than that of the crystal ($\rho_{crystal} < \rho_{liquid}$). Foremost example is of course water−ice. Nonreversible p-induced amorphization of crystalline into glassy ice has been reported[19,21] at $T = -196$ °C, i.e., far below the atmospheric T_m (0 °C). This is being explained by the isothermal p pathway at −196 °C traversing the p, T water−ice phase line, such as is pertinent near ambient conditions, but extrapolated to such low-T and high-p values where otherwise different crystal forms of ice are stable and hence where the water (here in a glassy form) is metastable (see Figure 13b in ref 2). The reason for this amorphization clearly lies in the inverted density relation of water and ice, which is supposed to pertain over the full range of p and T under consideration.

(ii) In the second source of p-induced amorphization invoked to explain amorphization, among others, in silicates,[18] the phase densities are in the customary relation, i.e $\rho_{crystal} > \rho_{liquid}$, at atmospheric and moderate pressures in the full T range in question, and hence the normal, positive dT_m/dp is observed. However, at high pressures, an inversion of densities is envisaged, with a corresponding sign inversion in dT_m/dp, by the Clausius−Clapeyron relation. This is equivalent to a change from region I to region II in the present work except that in the silicate works[18] it is not actually observed, but merely hypothesized. The actually observed pressure induced amorphization would then correspond to the isothermal crossing of the p, V line such as in region II. As, however, in those silicate cases no region III (hence re-entrant melting) is envisaged, the traversing of phase lines at ambient T is necessarily at very high p values such as correspond to the extension of the p, T line in region II down to room T, which in the case of silicates is reported to be the observation (see Figure 13a in ref 2).

The amorphization in our present case of P4MP1 (along pathway 1) has features in common with both points i and ii above but corresponds to neither. It possesses the inverted density relation $\rho_{crystal} < \rho_{liquid}$ under ambient conditions, just as in the water−ice system, but here ∼200 °C below the atmospheric T_m. When heated at low (including atmospheric) p, the densities cross over to the more usual relation of $\rho_{crystal} > \rho_{liquid}$, hence giving the conventional behavior on actual melting at T_m, i.e., a positive dT_m/dp. Consequently, the actual melting behavior cannot be simply transposed to the much lower T region where pressure induced amorphization (along pathway 1) is observed, as has been done for water−ice.[19−22] It is true that the inverted density, i.e., $\rho_{crystal} < \rho_{liquid}$, relation does set in also in the upper melt region, but only at high enough pressure values (sign inversion in the Clausius−Clapeyron relation—our region II) just as envisaged for silicates,[18] but as we have noted, this cannot be extrapolated down to room T in order to account for the amorphization of P4MP1, as along pathway 1, because the amorphization would only set in at a much higher pressure than actually observed. It appears therefore that the pressure-induced amorphization which ourselves are observing would correspond to the pattern of T_m depression behavior (with p) such as displayed by ice. But in the P4MP1 system only at ∼200 °C below the actual T_m, where the inverted density relation $\rho_{crystal} < \rho_{liquid}$ holds, is the atmospheric melting of such systems (in contrast to water−ice) unrealizable.

In addition to its scientific interest for phase behavior in general, amorphization by pressure, thus bypassing the requirement of high T and the presence of a liquid state of matter, should evidently be of potential interest for materials application. This is because it represents a distinct state of matter, which should have distinct properties of its own yet to be explored. This applies irrespective as to whether such a state of matter is created on purpose or whether it arises accidentally on applications such as involve (even if only local) pressures. In this respect reversibility, or otherwise, should be of crucial consequence. If reversible, the special properties of the amorphized phase will only pertain while the pressure is being applied. If irreversible, then the material is being permanently changed, thus becoming available for whatever use it may be suited.

Finally, there is the important issue of the structure of the "amorphized" material on a molecular level. Is it the same as, or does it differ from, that of a conventional melt? With the qualifications in section 4.1 we have taken that (vitrification apart) thermodynamically the two are equivalent at least for the purposes of the Discussion. How far this also holds in fine structural detail down to the molecular level remains a further question. We anticipate shedding light on this issue by work currently in progress.

Acknowledgment. The authors would like to thank Professor Jan Schouten of van der Waals Zeeman laboratory, University of Amsterdam, for providing the Raman spectroscopy facilities. Further, the authors are grateful for the availability of the X-ray facilities at beamline ID11/BL2 of the European Synchrotron Radiation Facility (ESRF), Grenoble, France. In particular, the support of Dr. Heinz Graafsma during the experiments is acknowledged together with the assistance of Dr. Andy Hammersley in the analysis of the X-ray data with the help of the FIT2D software program, developed at ESRF. The authors wish to thank Professor Robert Evans of the University of Bristol for stimulating discussions through out this work and specifically for his judgment and guidance on the conceptual issues arising in this paper. The high-pressure DSC measurements were supported by the Deutsche Forschungsgemeinschaft (SFB 239, University of Ulm), which is gratefully acknowledged. The authors are thankful to Professor Bernard Wunderlich (University of Tennessee) for useful critical comments.

Appendix

On the Fecht Scheme for Creating Melt Re-entry. The Scheme. Here some particulars will be provided on the Fecht scheme again, as in the main text, in our own formulation. To follow it, we have included Figure 8 in this paper from ref 16.

As a starting point we take Figure 1 of ref 16, which is our Figure 8a. This is a plot of free energy change, ΔG, normalized with respect to heat of fusion (ΔH_f), as a function of T, normalized with respect to the melting point (T_m), over the full T range beneath T_m, i.e., over the whole undercooling range for some "ideal intermetallic compound". For a defect-free crystal, first $\Delta G/H_f$ increases with decreasing T/T_m, passes through a maximum ,and then decreases on further decrease of T/T_m. While Fecht does not comment on it explicitly, it is clear that this course of the $\Delta G/H_f$ curve is due to the faster decrease of S_{liquid} compared to $S_{crystal}$ leading to a crossing over of the respective S vs T curves. Also it is obvious, but not explicitly stated in ref 16, that this leads to two intersections with the T/T_m line (the abscissa of Figure 8a): one at $T/T_m = 1$, the usual crystal melting point, and another at a much lower T. The relevant dashed line representing the downward portion of the $\Delta G/H_f$ line is not extended so far in Figure 8a. Nevertheless this lower intersection is very relevant for our purpose, because this second lower T_m signals the existence of a re-entrant melt phase region, such as foreseen by Tammann (not referred to in ref 16) which is our concern here. This melt re-entry is clearly the consequence of the shape of the $\Delta G/H_f$ curve, which, in turn, involves the validity of the Kauzmann paradox.

In what follows, Fecht introduces the restriction imposed by the Kauzmann paradox according to which S_{liquid} should not become smaller than $S_{crystal}$. Thus, going downward in T, we reach the temperature T_{go} where S_{liquid} becomes equal to $S_{crystal}$. On further lowering of T, S_{liquid} remains equal to $S_{crystal}$. As by Kauzmann,[15] below T_{go}, H_{liquid} should vary in the same way as $H_{crystal}$ (the respective H vs T lines remain parallel) it follows that the $\Delta G/H_f$ line in Fecht's Figure 1 remains constant on lowering of T below T_{go}. In other words, the decrease of ΔG with decreasing T is avoided and with it the existence of a re-entrant melt phase in an ideal

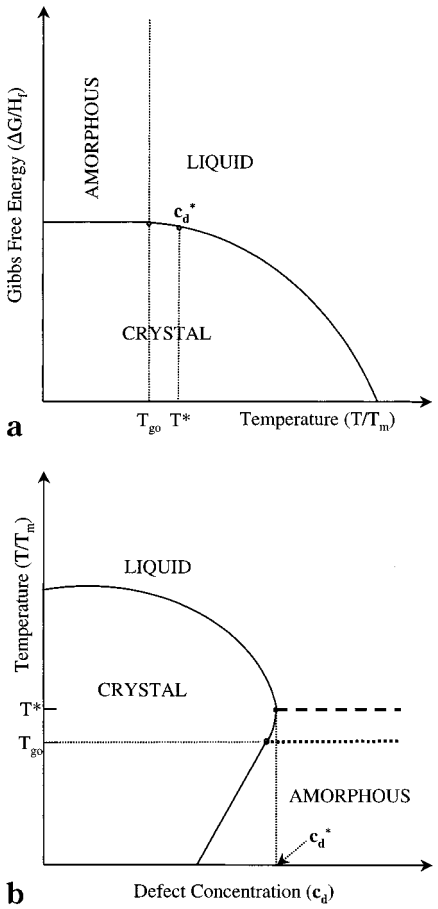

Figure 8. (a) Gibbs free energy difference between the undercooled liquid and ideal single crystalline compound. The undercooled liquid is distinguished from the amorphous solid by the ideal glass transition temperature. (b) Universal melting diagram representing three nonequilibrium states, the crystal supersaturated with defects, the undercooled liquid and amorphous solid. (for detail see ref 16). Reproduced from Figure 1 in ref 16. Copyright 1988 Nature.

perfect crystal. As will be recognized, T_{go} is the usually invoked "ideal glass transition temperature", which by conventional vitrification considerations can only be approached but never fully attained.

Thus, having eliminated melt phase re-entry for an ideal crystal, Fecht reintroduces it again by invoking defected crystals in a state of metastable equilibrium (the main issue of his work) while retaining the Kauzmann paradox. He considers defected crystals with an externally variable defect concentration (c_d, our notation; the specific case he quotes is the vacancy concentration in metals which can be controllably created by (γ -irradiation). Further, it is postulated that this defect concentration is frozen in, creating a metastable state, which can then be compared with the corresponding molten state (liquid or glass according to T) at the same T for considerations of phase stability. This leads to an increase in the free energy difference ΔG^* between crystal and melt in excess to that pertaining for the defect free crystal. Here this incremental ΔG^* (due to defects) is taken to have a (negative) T coefficient which is an increasing function of c_d. Now, an inspection of Figure 8a will show, with the defected crystal of a particular defect content (c_d) serving as a reference (i.e. $\Delta G^* = 0$), that there can again be two intersections of the $\Delta G/H_f$ lines, with the now renormalized abscissa T/T_m (corresponding to $\Delta G^* = 0$). Even the restriction

imposed by the Kauzmann paradox (as relating to the ideal crystal) is incorporated. For details see ref 16.

The points of intersection (i.e., T_m values) in Figure 1 of ref 16, when plotted against c_d, yield the T, c_d "phase" diagram (Figure 8b). This has the same features as our p, T diagram in our Figure 7 from region II onward (i.e., from p_q). This comprises a decrease in T_m with c_d up to an extreme point (such as r in our case with a corresponding $T = T^*$) where the phase line starts curving back on itself leading to a double valued T_m, i.e., to melt phase re-entry. The extreme point (termed "nose" by Fecht) corresponds to $\Delta H = \Delta S = 0$ as stated by Tammann back in 1903. In addition, however, the influence of vitrification at T_{go} is reflected by the phase line. From here on, we refer the reader back to the main text.

Critique. Three questions/critiques can be raised in connection with the Fecht scheme presented above.

(1) The first is the taking of the defected crystal as a frozen in, locally stable (hence a metastable) state, which can then serve as a reference for thermodynamic equilibrium considerations. This is an issue of the kind that arises in a variety of phase transition problems. Besides pointing it out, we do not attempt to provide an answer. No doubt each case needs to be taken on its own merit with the time scale on which the metastable system can be regarded as stable being the determining factor.

(2) The second is the incorporation of vitrification (T_{go}), specifically its influence on phase transitions, into an actual phase diagram. For this we need to bear in mind that basically vitrification is a kinetic (i.e., time scale dependent) phenomenon and not a thermodynamic effect. This is a deep-seated issue subject to much debate relating to the glassy state in general (e.g., the existence of a true T_{go}, etc.) to which we have no further comment at this point.

(3) The last is the taking of the ideal (i.e., defect-free) crystal as the basis for defining T_{go}, even in relation to the defected crystal. In contrast to points 1 and 2 above, which have wider pertinence for metastable and vitrified systems in general, this particular reservation is specific to the Fecht scheme as such. (We are indebted to Prof. Robert Evans, University of Bristol. for having drawn our attention to this issue.)

Strictly speaking one would need a different T_{go} for each defect content, which would affect the starting point and the slope of the $\Delta G/H_f$ line below the appropriate T_{go} for the particular defected crystal (Figure 8a). Thus, the "phase diagram" is bound to be affected by such a redefinition of T_{go}, but how far it would still retain its present qualitative features, our main concern here, we cannot say at present. For a definitive assessment of the Fecht scheme, this issue would require separate attention.

References and Notes

(1) Rastogi, S.; Newman, M.; Keller, A. *Nature* **1991**, *353*, 55.
(2) Rastogi, S., Newman, M.; Keller, A. *J. Polym. Sci. (Polym. Phys.)* **1993**, *B31*, 125.
(3) Höhne, G. W. H.; Rastogi, S.; Wunderlich, B. Polymer (to appear in the special issue dedicated to Prof. A. Keller in 2000).
(4) Blankenhorn, K.; Höhne, G. W. H. *Thermochim. Acta* **1991**, *187*, 219. Höhne G. W. H.; et al. *Thermochim. Acta* **1996**, *273*, 17.
(5) Zoller, P. J. *Appl. Polym. Sci.* **1977**, *21*, 3129.
(6) Griffith, J. H.; Ranby, B. G. *J. Polym. Sci.* **1960**, *XLIV*, 369.
(7) Gabba, S. M.; Stivala, S. S. *Polymer* **1976**, *17*, 121.
(8) Bahuguna, G. P.; Rastogi, S.; Tandon, P.; Gupta, V. D. *Polymer* **1996**, *37*, 745.
(9) Jain, P. C.; Wunderlich, B.; Chaubey, D. R. *J. Polym. Sci., (Polym. Phys.)* **1977**, *15*, 2271.
(10) Okumura, S.; Miyaji, H.; Izumi, K.; Toda, A.; Miyamoto, Y. *Polymer* **1996**, *11*, 2285.
(11) Zoller, P.; Starkweather, H. W. *J. Polym. Sci. (Polym. Phys.)* **1986**, *B24*, 1451.
(12) Tammann, G. *Kristallisieren und Schmelzen*; Verlag Johann Ambrosius Barth: Leipzig, Germany, 1903.
(13) Tammann, G.; Mehl, R. F. *The States of Aggregation*; Van Nostrand Co.: New York, 1925. Ricci, J. E. *The Phase Rule & Heterogeneous Equilibrium*; Dover Publication Inc.: London 1966.
(14) Vogel, R. *Die Heterogene Gleichgewichte*, 2nd ed.; Akademische Verlagsgesellschaft: Leipzig, Germany, 1959.
(15) Kauzmann, W. *Chem. Rev.* **1948**, *43*, 219.
(16) Fecht, H. J. *Nature* **1992**, *356*, 133. Fecht, H. J.; Johnson, W. L. *Nature* **1988**, *334*, 50.
(17) Highmore, R. J.; Greer, A. L. *Nature* **1989**, *339*, 363. Greer, A. L. *J. Less Common Met.* **1988**, *140*, 327.
(18) Hemley, R. J.; Jephcoat, A. P.; Mao, H. K.; Ming, L. C.; Manghnani, M. H. *Nature* **1988**, *334*, 52.
(19) Mishima, O.; Calvert, L. D.; Whalley, E. *Nature* **1984**, *310*, 393.
(20) Hemley, R. J.; Chen, L. C.; Mao, H. K. *Nature* **1989**, *338*, 638.
(21) Mishima, O.; Calvert, L. D.; Whalley, E. *Nature* **1985**, *314*, 76.
(22) Whalley, E.; Klug, D. D.; Handa, Y. P. *Nature* **1989**, *342*, 782.
(23) Jayaraman, A.; Wood, D. L.; Maines, R. G. *Phys. Rev.* **1987**, **B35**, 8316.
(24) Williams, Q.; Jeanloz, R. *Science* **1988**, *239*, 902.
(25) Kruger, M. B.; Jeanloz, R. *Science* **1990**, *249*, 647.
(26) The relevant parts of the first German language publication of ref 12 is recapitulated in a later English version, ref 13, which, however, while containing much else, does not treat this particular issue in quite the same depth. We also found it instructively recapitulated in a later textbook by Vogel on phase equilibria.[14]
(27) Such an example was benzophenone. It would be interesting to check whether or not this has been verified by experimental works since. If not, it could be instructive to undertake such a work at the present date.

MA9912958